Avalanche Excitations of Fast Particles in Quasi-2D Cold Dusty-Plasma Liquids

Ying-Ju Lai and Lin I

Department of Physics, National Central University, Chungli, Taiwan 32054, Republic of China

(Received 16 May 2002; published 18 September 2002)

We study the spatiotemporal cooperative microexcitations in quasi-2D cold dusty-plasma liquids from the view of the coupled subexcitable nonlinear dynamical system. Under the interplay of thermal noise and mutual coupling, cooperative fast-particle clusters are excited in the *xyt* space. The fast hopping plays a major role in the superdiffusion with non-Gaussian velocity distribution and causes the loss of bond-orientation memory. The size distribution of the excited clusters in the *xyt* space follows a similar avalanche-type power-law relation as in other subexcitable systems.

DOI: 10.1103/PhysRevLett.89.155002 PACS numbers: 52.27.Lw, 05.40.–a, 64.60.Cn

The dynamical behavior of the nonlinear subexcitable spatiotemporal system under noise is an interesting problem. Although noise might have disruptive effect, it also shows constructive influence and induces spatiotemporal coherence, especially enhanced under spatial coupling. Noise-induced spatiotemporal excitations have been observed in a large variety of physical, chemical, and biological systems [1–6], similar to the noise-enhanced signal in temporal systems through stochastic resonance. Pulses in diode array and subexcitable media [1,2], avalanche excitation of spiral waves in Belousov-Zhabotinsky (BZ) reaction [4], and waves in a cultured network of rat brain cells [5] are a few good examples.

Similarly, a liquid is also a coupled many-body system under thermal fluctuations. Regardless of its disordered long time micromotion, whether the noise can also induce coherent excitations of microstructure and motion at the time scale shorter than the thermal equilibrium time and their generic statistical spatiotemporal behaviors are interesting open issues. In this Letter, from the point of the noise-induced coherence in subexcitable dynamical systems, we address this issue experimentally using a cold quasi-2D dust Coulomb liquid in a dusty-plasma system.

In dusty plasmas, micrometer size dust particles can be suspended and self-organized into crystal or liquid structures [7,8]. The strong Coulomb coupling is induced by strong negative charging (about 10^4 electrons per particle) from the gaseous discharges. Through direct visualization, it provides a platform to understand many generic features of the strongly coupled Coulomb system under very low viscous damping by the low pressure neutral gas (10^2 m Torr). The formation of dusty-plasma crystals, liquids, and clusters, lattice waves, melting, defect formation, etc., are examples studied in recent years [7–13]. The thermally excited microdynamics in liquids has been less well explored.

Figure 1 shows the typical particle motions in our quasi-2D dusty-plasma liquid. Unlike the small amplitude caged oscillation in the triangular lattice site for the crystal state under the strong Coulomb coupling, the stronger thermal noise can drive disordered long time motion [Figs. 1(a) and 1(b)]. However, at the short time scale [Figs. 1(c) and 1(d)], temporally ordered domains with triangular structure coexist with hopping strings or vortices. Namely, particles alternately exhibit small amplitude caged oscillation in the temporally ordered domains and cooperative hopping. Cooperative fast-particle motions have also been observed experimentally in the melting transition of 2D dusty plasmas [9] and in the 2D and 3D liquids or glass transition of other systems [14,15]. The fast hopping motion is not fully thermalized and causes non-Gaussian velocity distributions at the short time scale [14,15]. For motion, we can treat the fast particle as in the state excited from the quiet caged motion by noise. The excited region can relax back to the quiet ordered triangular lattice structure. Structurally, hopping causes lattice distortion and, in turn, the cooperative excitations of defect sites losing bond-orientational order (BOO), also in the form of clusters in *xy* space [Fig. 1(f)] [12,13]. We can measure the local BOO, $\psi_6(r) = \frac{1}{N_r}\sum_i \exp(i6\theta_i)$, where θ_i is the angle of the vector from the particle at r to its ith nearest neighbor, and N_i is the number of the nearest neighbors [16]. $|\psi_6| = 1$ at the perfect sixfold lattice sites and <0.4 for the defect sites, respectively [17]. Noise plays two roles under mutual coupling: (i) Initiating local excitations through the local accumulation of favorable perturbation and (ii) supporting as well as breaking the cascaded spatiotemporal propagation of cooperative excitations in *xyt* space as a percolation process [4]. Namely, the cooperative excitation events also appear in the form of clusters with various sizes in *xyt* space.

In this Letter, we identify the fast particles and their roles on non-Gaussian dynamics and BOO temporal correlation, which have never been studied in the cold 2D dusty-plasma liquids. We then test whether the general concept of the noise-induced coherence for subexcitable systems can be applied to understand and characterize the spatiotemporal behaviors of cooperative excitations, which to our knowledge, have never been addressed in liquid systems. It is found that the fast particles in the non-Gaussian velocity distribution tail lead to the

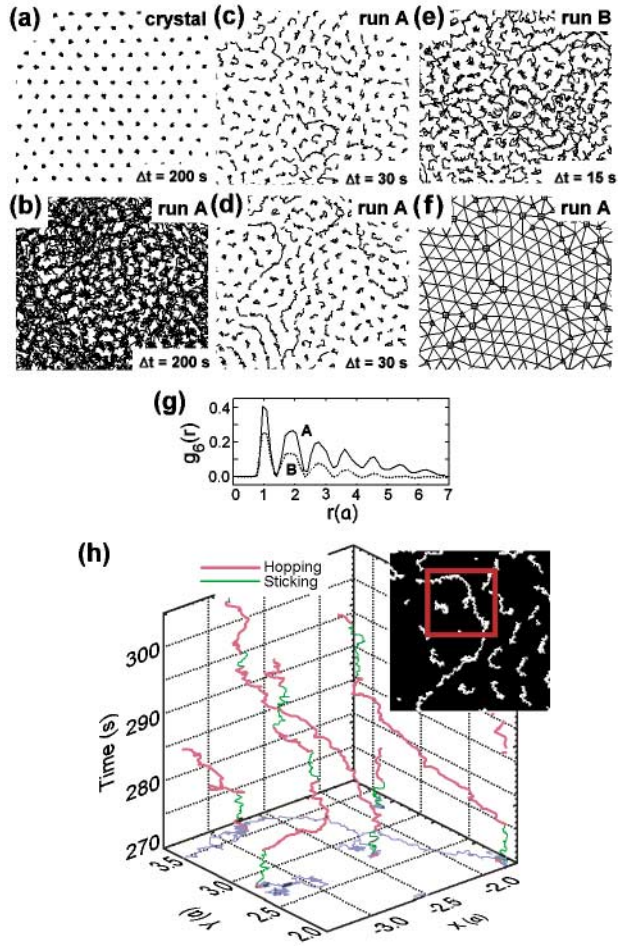

FIG. 1 (color). (a) and (b) Typical long time particle trajectories for the crystal and the cold liquid state (run *A*), respectively. (c) and (d) The typical short time trajectory plots showing the alternate caged oscillation and the cooperative hopping in the form of strings and vortices for run *A*. (e) The short time motion for the hotter run *B*. (f) The triangular plot of a snapshot of particle positions for run *A*. The triangles and squares correspond to the five- and sevenfold defects, where the lattice is serious distorted with BOO < 0.4. (g) The radial pair correlation function of BOO for runs *A* and *B*. (h) The 3D *xyt* trajectory of run *A* corresponding to the particles in the red box of the upper right 2D plot which is magnified from the upper left corner of (d). The red and green trajectories correspond to the hopping and caged states, respectively, and the blue lines are the corresponding projections on the *xy* plane.

transition from the caged subdiffusion regime to the hopping dominated superdiffusion regime associated with the memory loss of BOO, and eventually to the normal diffusion regime after accumulation of many hoppings at long time scale. The size distributions of the excitation clusters in the *xyt* space follow the generic self-organized criticality avalanche-type power-law relation, similar to the photonoise-induced cooperative excitations in the 2D BZ reaction system [4,18].

The experiment is conducted in a cylindrical symmetric rf dusty-plasma system described elsewhere [12]. A weakly ionized discharge ($n_e \sim 10^9$ cm^{-3}) is generated in 250 mTorr Ar gas using a 14 MHz rf power system. A hollow cylindrical cell 30 mm in diameter is placed on the center of the bottom electrode to trap polystyrene particles at 7 μm diameter. Vertically, the suspended dust particles are aligned with eight particles for each chain by the vertical ion flow-induced dipoles. Particles in the same vertical chain move together horizontally for the liquid states in our studies. It forms a quasi-2D system. Illuminated by a thin horizontal laser sheet, the particle (vertical chain) positions in the horizontal plane are monitored through digital video optical microscopy. The mean interparticle distance a is 0.3 mm. Regardless of the complicated heating mechanism for dusty plasmas, we can increase the degree of disorder by increasing the rf power. A cold liquid state after melting (run *A*, obtained at 1.8 W rf power) and another hotter liquid state (run *B*, obtained at 2.4 W rf power) are used as examples in this study. Fifty series of picture frames each with 150 sec length and 400 particles in each frame are used for statistical measures.

Figures 1(b)–1(f) show the typical trajectories and the typical triangular structure with defects for run *A* and *B*. The temporally ordered domains with a few a scales coexist with the active hopping strings or vortices. It causes a few a correlation lengths of BOO in Fig. 1(g), where the radial correlation function of BOO, $g_6(r) = \langle \psi_6(0)^* \psi_6(r) \rangle$, for runs *A* and *B* are plotted.

Figures 2(a)–2(c) show the particle displacement histograms at different time interval τ and the non-Gaussian parameter, $\alpha_2 = \langle \Delta R^4 \rangle / 2 \langle \Delta R^2 \rangle^2 - 1$, which measures the deviation of the displacement distribution from a random Gaussian distribution. For a Gaussian distribution, the $\log P(\Delta R^2)$ versus ΔR^2 plot should follow a straight line. Figures 2(d) and 2(e) show the time dependence of particle mean square displacement, MSD $= \langle \Delta R^2 \rangle$, and the temporal correlations of BOO, $g_6(\tau) = \langle \psi^*(\tau) \psi(0) \rangle$, averaged after trailing each particle temporally.

The 3D *xyt* trajectory plot of the cold run *A* in Fig. 1(h) provides a clear microscopic picture for the temporal behaviors in Fig. 2. At very short time ($< \tau_1$, where $\tau_1 =$ 1.9 and 0.5 sec for runs *A* and *B*, respectively), the motion is dominated by the transient caging effect from the neighboring particles and mainly exhibits high rate small amplitude oscillation. It causes the subdiffusion with the exponent α of MSD (i.e., MSD $\propto \tau^\alpha$) smaller than 1. BOO shows good temporal correlation because the relative particle position (i.e., the bond orientation) is only slightly changed within τ_1. For the intermediate time scale ($\geq \tau_1$), the displacement is dominated by the stick-slip type persistent hopping (red lines) between the caging states (green lines). It switches the transition from the subdiffusion to the superdiffusion regime with $\alpha > 1$ at $\tau = \tau_1$, where α_2 reaches the maximum. The displacement histograms in Figs. 2(a) and 2(b) show the

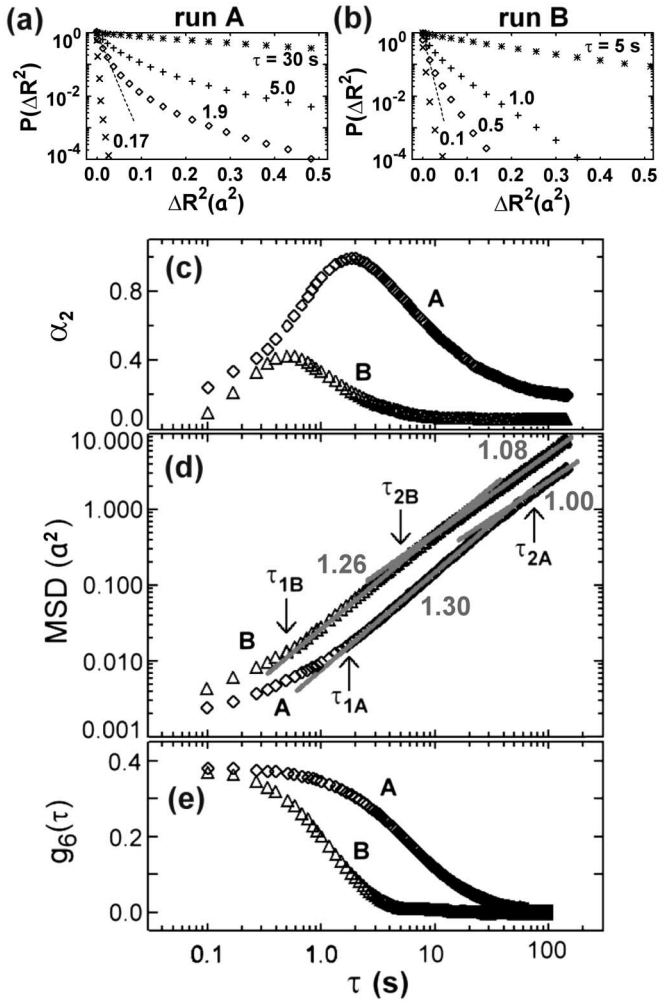

FIG. 2. (a) and (b) The histograms of the particle square displacement $P(\Delta R^2)$ for runs A and B. The two straight lines are the best Gaussian fit for runs A and B at $\tau = 1.9$ and 0.5 sec, respectively. The upward bending histograms deviated from the straight lines indicate the contribution from the nonequilibrium fast hopping particles. (c) to (e) The temporal dependences of α_2, MSD, and $g_6(\tau)$ for runs A and B. τ_1 and τ_2 correspond to the onsets of the transitions to the superdiffusion and the normal diffusion, respectively. The gray lines and the nearby numbers in the MSD plots correspond to the best fits and the exponents, respectively.

most serious non-Gaussian upward bending at τ_1 (e.g., 1.9 sec for run A). Namely, at τ_1, the motion is still far from thermal equilibrium. The onset of hopping dominated transition also starts to induce position rearrangement and causes the onset of memory loss for BOO. Eventually, the displacement is randomized by the accumulation of many random phased hopping cycles at very large $\tau(> \tau_2)$. It leads the diffusion back to normal with $\alpha \simeq 1$, the displacement histogram to Gaussian [see the straight long time histograms in Figs. 2(a) and 2(b)], and the serious memory loss of BOO. In run B [Fig. 1(e)], under the higher thermal noise, particle motions become more violent with faster hopping mixing, which shortens the time scale for all the transitions and decreases the peak value of α_2 (Fig. 2). Note that our above three-stage diffusion behavior is similar to that found at the melting transition of the 2D dusty-plasma crystal [9].

We now focus on the statistical behaviors of the persistent fast particles. The particles with displacement greater than the half-width of the displacement in τ_1, and the angle between the two successive displacement vectors (separated τ_1 apart) smaller than 70°, are defined as persistent fast particles. The histogram of the starting to the end traveling distance of the fast persistent motion,

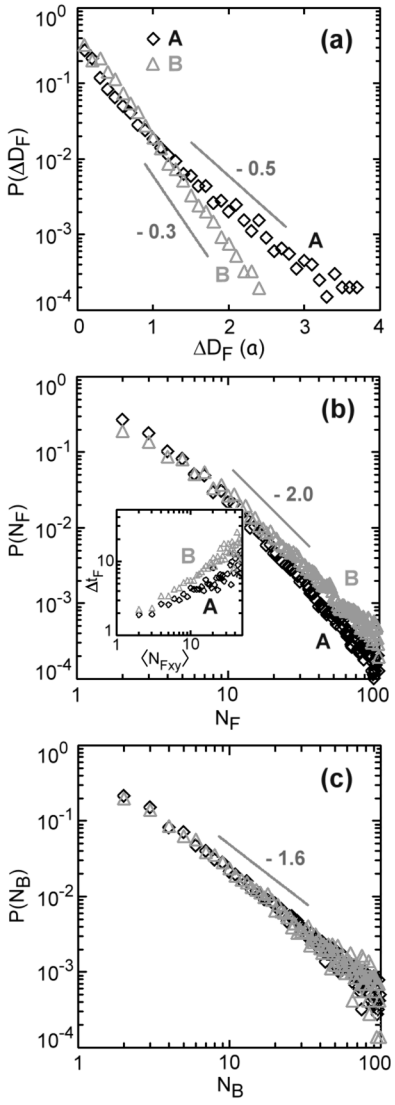

FIG. 3. (a) The histograms of ΔD_F for runs A and B. (b) The histograms of N_F normalized by the total number of clusters in the xyt space. The inset shows power-law relation between the temporal span Δt_F and the averaged spatial span $\langle N_{Fxy}\rangle = \langle N_F/\Delta t_F\rangle$ of the fast-particle clusters. (c) The histograms of N_B. The number nearby each gray line corresponds to its exponent.

ΔD_F, in xy plane trailing individual particle, nearly follows an exponential distribution [Fig. 3(a)] with decay width in the order of $0.5a$. Namely, after excitations, regardless of the few events persisting fast motion up to a few a, most of the fast particles persist less than $1a$ and reenter the quiet caged state. The higher noise level of the hotter run B slightly shortens the persistent traveling distance. Figure 3(b) shows the normalized histogram of N_F, the number of the connected cooperative fast events of a cluster in the xyt space. Both runs A and B show power-law relation with a scaling exponent about -2. The histograms of N_B, the normalized number of the connected BOO excitation events (i.e., $|\langle\psi_6\rangle| < 0.4$) in the xyt space, also show power-law relation with a scaling exponent $= -1.6$ for both runs [Fig. 3(c)]. Note that the power-law distribution of the fast-particle number in the xyz space was observed in the 3D supercooled colloidal suspensions, but without temporal measure [15]. The inset in Fig. 3(b) plots the power-law relation between the time span Δt_F and the averaged spatial size $\langle N_{F_{xy}}\rangle = \langle N_F/\Delta t_F\rangle$ of fast-particle clusters. The exponents equal 0.57 and 0.75 for runs A and B, respectively. The longer-life cluster involves more particles simultaneously hopping together.

Noise induces particle relative displacement and, in turn, increases the local strain energy through Coulomb coupling. Hopping starts after sufficient accumulation of multiple constructive perturbations either from local noise or local strain. Namely, it depends on the histories of the noise and the states of the particle and its neighboring particles. On one hand, the Coulomb coupling makes particles form an ordered lattice. On the other hand, it transfers the kinetic energy of a fast particle to the surrounding particles and further induces their cascaded hoppings. If the constructive perturbation cannot be continuously supplied, hopping ceases. It is more difficult to make a large area region simultaneously and persistently under constructive perturbation to excite large clusters in xyt space. The observed spatiotemporal scaling relations (e.g., with exponent about -0.20) without a typical scale is quite similar to that observed in the noise-induced excitation in the 2D BZ reaction system [4]. It manifests that the nucleationlike cooperative excitation process is akin to the avalanche behavior in self-organized criticality [18].

In conclusion, we demonstrate that, under the interplay between thermal fluctuations and Coulomb coupling, the avalanche-type microexcitation in our cold quasi-2D dusty-plasma liquids is a new paradigm of the noise-induced coherence in coupled subexcitable nonlinear dynamical systems. The excitations of fast particles play a major role to induce a large non-Gaussian parameter for particle motion and the onset of superdiffusion at the short time scale. It also affects the dynamics of BOO and induces its memory loss through position rearrangement. The cooperatively excited sites appear in the form of clusters in the xyt space. Their cluster size distributions follow power-law relation with exponents about -2.0 and -1.6, respectively. The cooperative excitation with larger spatial span lasts a longer time.

This research is supported by the National Science Council of the Republic of China under Contract No. NSC-90-2112-M008-50.

[1] M. Locher, D. Cigna, and E. R. Hunt, Phys. Rev. Lett. **80**, 5212 (1998).
[2] H. Hempel, L. Schimansky-Geir, and J. Garcia-Ojalvo, Phys. Rev. Lett. **82**, 3713 (1999).
[3] J. F. Linder *et al.*, Phys. Rev. Lett. **75**, 3 (1995).
[4] J. Wang, S. Kadar, P. Jung, and K. Showalter, Phys. Rev. Lett. **82**, 855 (1999).
[5] P. Jung, A. Cornell-Bell, K. S. Madden, and F. Moss, J. Neurophysiol. **79**, 1098 (1998).
[6] C. Van den Broeck, J. M. R. Parrondo, and R. Toral, Phys. Rev. Lett. **73**, 3395 (1994).
[7] J. H. Chu and Lin I, Phys. Rev. Lett. **72**, 4009 (1994).
[8] H. Thomas *et al.*, Phys. Rev. Lett. **73**, 652 (1994).
[9] Lin I, W. T. Juan, C. H. Chiang, and J. H. Chu, Science **272**, 1626 (1996); W. T. Juan and Lin I, Phys. Rev. Lett. **80**, 3073 (1998).
[10] J. B. Pieper and J. Goree, Phys. Rev. Lett. **77**, 3137 (1996).
[11] J. Pramanik, G. Prasad, A. Sen, and P. K. Kaw, Phys. Rev. Lett. **88**, 175001 (2002).
[12] W. T. Juan *et al.*, Phys. Rev. E **58**, R6947 (1998); Y. J. Lai and Lin I, Phys. Rev. E **64**, 015601(R) (2001).
[13] A. Melzer, A. Homann, and A. Piel, Phys. Rev. E **53**, 2757 (1996); R. A. Quinn and J. Goree, Phys. Rev. E **64**, 051404 (2001).
[14] For example, K. Zahn and G. Maret, Phys. Rev. Lett. **85**, 3656 (2000); W. K. Kegel and A. van Blaaderen, Science **287**, 290 (2000).
[15] E. R. Weeks, J. C. Crocker, A. C. Levitt, A. Schofield, and D. A. Weitz, Science **287**, 627 (2001).
[16] K. J. Strandburg, *Bond-Orientational Order in Condensed Matter Systems* (Springer, New York, 1992).
[17] Y. J. Lai, Ph.D. thesis, National Central University, Republic of China, 2002.
[18] For example, P. Bak, C. Tang, and K. Wiesenfeld, Phys. Rev. Lett. **59**, 381 (1987); H. J. Jensen, *Self-Organized Criticality* (Cambridge University, Cambridge, 1998).